Minimum Energy Control of an S-CVT Equipped Power Transmission

Jungyun Kim*
School of Mechanical and Aerospace Engineering, Seoul National University, Seoul 151-742, Korea

This article deals with a minimum energy control law of S-CVT connected to a dc motor. The S-CVT can smoothly transit between the forward, neutral, and reverse states without any brakes or clutches, and its compact and simple design and its relatively simple control make it particularly effective for mechanical systems in which excessively large torques are not required. And such an S-CVT equipped power transmission has the advantage of being able to operate the power sources in their regions of maximum efficiency, thereby improving the energy efficiency of the transmission system. The S-CVT was intended to primarily for use in small power capacity transmissions, thus a dc motor was considered here as the power source. We first review the structure and operating principles of the S-CVT, including experimental results of its performance. And then we describe a minimum energy control law of S-CVT connected to a dc motor. To do this, we describe the results of an analysis of the dynamics of an S-CVT equipped power transmission and the power efficiency of a DC motor. The minimum energy control design is carried out via B-spline parameterization. And we show numerical results obtained from simulations illustrate the validity of our minimum energy control design, benchmarked with a computed torque control algorithm for S-CVT.

Key Words : Minimum Energy Control, S-CVT, B-Spline Parameterization, Computed Torque Control

1. Introduction

Continuously variable transmissions (CVTs) have been the object of considerable research interest within the mechanical design community, driven primarily by automotive applications. Unlike conventional stepped transmissions, a CVT allows for a continuous range of gear ratios that can, up to certain device-dependent physical limits, be selected independently of the applied torque. Among the various advantages of a CVT, the most prominent is its ability to run the power source at the power efficient regime. Furthermore, in most power sources such as internal combustion engines and electric motors, optimal efficiency lies at a certain operating point.

Therefore, many control engineers have been endeavoring to find an effective way of controlling a CVT's gear ratio to maintain the power source at the most efficient point and realize shifting commands in the desired manner (Takahashi, 1998 ; Heera and Hyunsoo, 2002). Optimal control of a CVT equipped power transmission is then defined as the problem of finding a gear ratio which can minimize the energy consumption of the power source without any losses in output performance. Hence, in order to design a minimum energy control law for a CVT, one must first investigate the efficiency characteristics of the power source as well as define the target performance. Driven mainly by automotive engi-

* **E-mail** : kjungyun@robotics.snu.ac.kr
TEL : +82-2-880-8050; **FAX** : +82-2-889-6205
School of Mechanical and Aerospace Engineering, Seoul National University, Seoul 151-742, Korea.
(Manuscript **Received** February 25, 2002; **Revised** October 21, 2003)

neers, various control approaches have been tried and realized. There are two major issues in controlling CVTs to achieve efficiency and performance objectives : power source consolidated control, and establishing the shifting map (the variogram), which is a look-up table of the speed relations between the power source and output.

In a previous study (Jungyun et al., 2002), we reported a novel CVT element, the spherical CVT (S-CVT) together with a kinematic and dynamic analysis of the device. The S-CVT has a simple kinematic structure, infinitely variable transmission (IVT) characteristics, and transmits power via dry rolling friction on the contact points between a sphere and discs. Its compact and simple design and relatively simple control make it particularly effective for mechanical systems in which excessively large torques are not required. The S-CVT is intended for use in small power capacity power transmissions ; thus a dc motor is considered as the power source in this study.

In this paper, we present a minimum energy control law for the S-CVT connected to a dc motor. Section 2 briefly reviews the design and operating principles of the S-CVT together with experimental results of its performance. In Section 3 we describe the equations of motion for the S-CVT equipped power transmission.

In addition, we investigate the general power efficiency characteristics of a dc motor using the well-known dc motor dynamic equations. Section 4 deals with the minimum energy control design via a B-spline parameterization of the trajectories. Finally we show some numerical results of energy savings using the proposed minimum energy control law. For benchmarking purpose, a computed torque control algorithm for the S-CVT is proposed taking into account the equations of motion of the S-CVT equipped power transmission system and an ideal motor model.

2. Spherical CVT

In this section a spherical continuously variable transmission (S-CVT) is described. The S-CVT is marked by its simple kinematic design and IVT characteristics, i.e., the ability to transit smoothly between the forward, neutral, and reverse states without the need for any brakes or clutches.

2.1 Structure and operating principles

The S-CVT is composed of three pairs of input and output discs, variators, and a sphere (see Fig. 1). The input discs are connected to the power source, e.g., an engine or an electric motor, while the output discs are connected to the output shafts. The sphere transmits power from the input discs to the output discs via rolling resistance between the discs and the sphere. The variators, which are connected to the shifting controller,

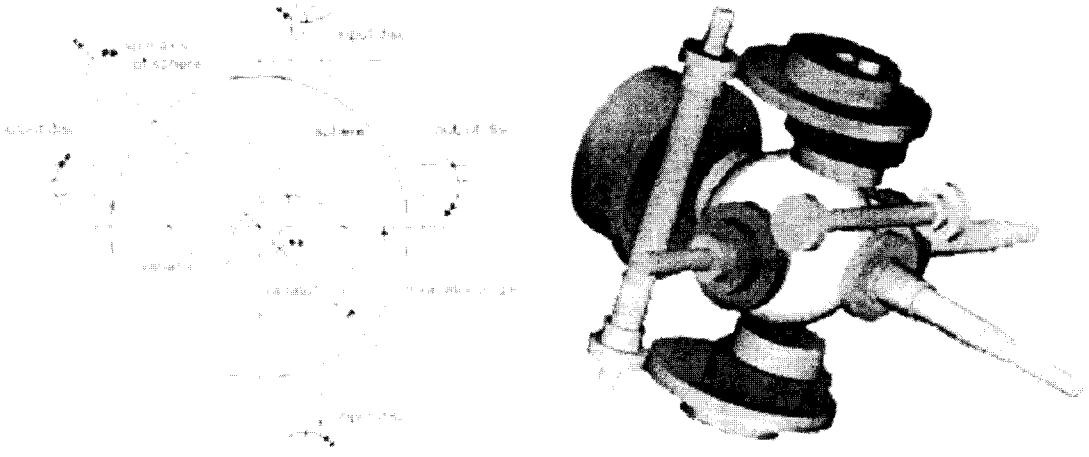

(a) Standard structure of S-CVT (b) 3-dimensional view

Fig. 1 Spherical CVT

are in contact with the sphere like the discs, and constrain the direction of rotation of the sphere to be tangent to the rotational axis of the variator. To transmit power from the discs to the sphere or from the sphere to the discs, a device that supplies a normal force to the sphere, such as a spring or hydraulic actuator, must be installed on each shaft.

By varying the axis of rotation of the sphere, it is in turn possible to vary the radius of rotation of the contact point between the input disc and the sphere, R_i, as well as the radius of rotation of the contact point between the output disc and the sphere, R_o (see Figure 2). In this way the speed-torque ratio of the S-CVT can be adjusted. Figure 2 shows the various alignments of the variator for the forward, neutral, and reverse states of the output shaft of the S-CVT. The neutral state, which corresponds to zero rotation of the output disc, is achieved when R_o becomes zero. As apparent from the figure, the forward, neutral, and reverse states can all be achieved by smoothly manipulating the variator alignment, without the need for any additional clutches or brakes.

Assuming roll contact without slip, the speed and torque ratio between the input and output discs is related to the variator angle by the following relations:

$$\frac{\omega_{out}}{\omega_{in}} = \frac{r_i}{r_o} \tan\theta \tag{1}$$

$$\frac{T_{out}}{T_{in}} = \frac{r_o}{r_i} \cot\theta \tag{2}$$

where θ is the angular displacement of the variator, ω_{in} and ω_{out} are the respective angular velocities of the input and output shafts, T_{in} and T_{out} are the respective input and output torques, and r_i and r_o are the respective radii of the contact points of the input and output discs (see Fig. 2).

2.2 Experimental results

In order to validate the operating principles and performance of the S-CVT, we have built a prototype and testbench for it (see Figure 3). Two eddy-current type AC servo motors (input: 3-phase AC, 122 V, 9 A; output: 1500 Watts; rated speed: 2000 rpm) are used for a driving

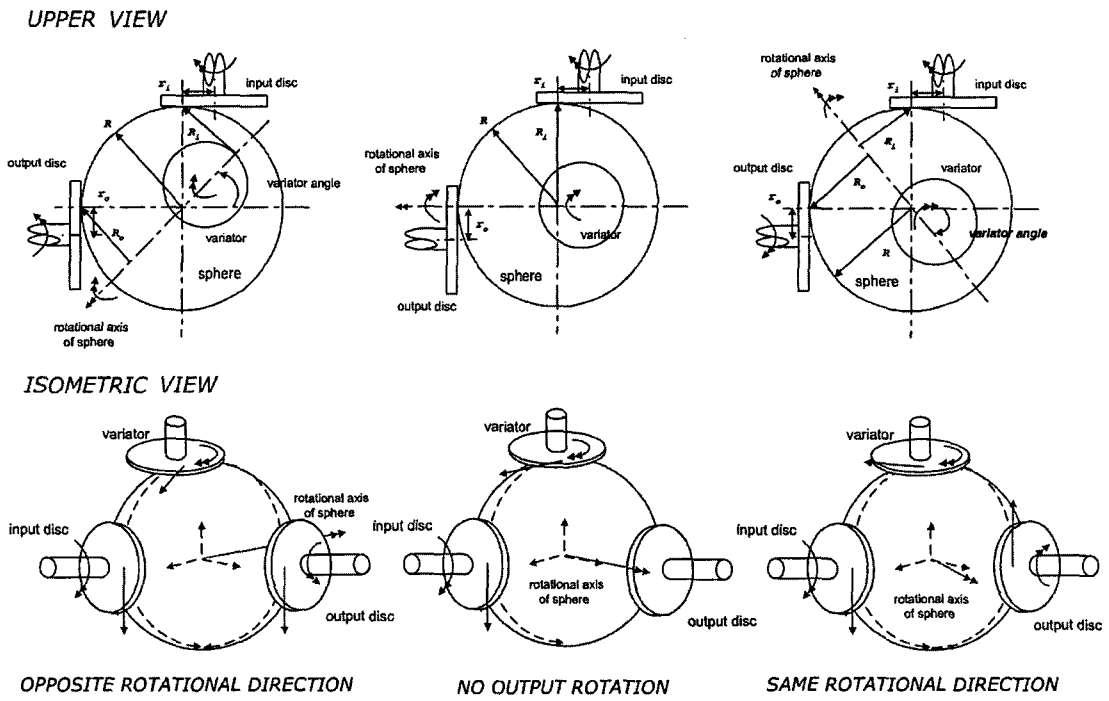

Fig. 2 Operating principles of S-CVT

power source and a driven load generator. In the testbench (see Fig. 3(b)), the variator angle is controlled by a dc stepped motor with an angular resolution of 0.024°/*pulse*. The rotational speeds of the input and output shafts are measured through incremental optical encoders attached to the shafts (see more details in Jungyun et al., 2002).

A steady-state speed ratio curve of the S-CVT is extracted for the no-load condition, when the input speed is set respectively to 748, 1502, and 2001 rpm (see Fig. 4(a)). And using slip-ring type torque sensors, we have also observed the output torque together with the variator angle displacement by adjusting input/output torque to realize the pre-obtained steady state speed ratio (see Figure 4(b)). The actual torque ratio is limited to under 20, which is determined mainly by the static coefficient of friction and the exerted normal force.

3. S-CVT Equipped Power Transmission

Because the S-CVT transmits power via rolling resistance between metal on metal, it has limitations on the overall transmitted torque, which is effectively determined by the static coefficient of friction and the magnitude of the normal forces applied to the sphere. Due to this torque limitation, target applications for the S-CVT include mobile robots, household electric appliances,

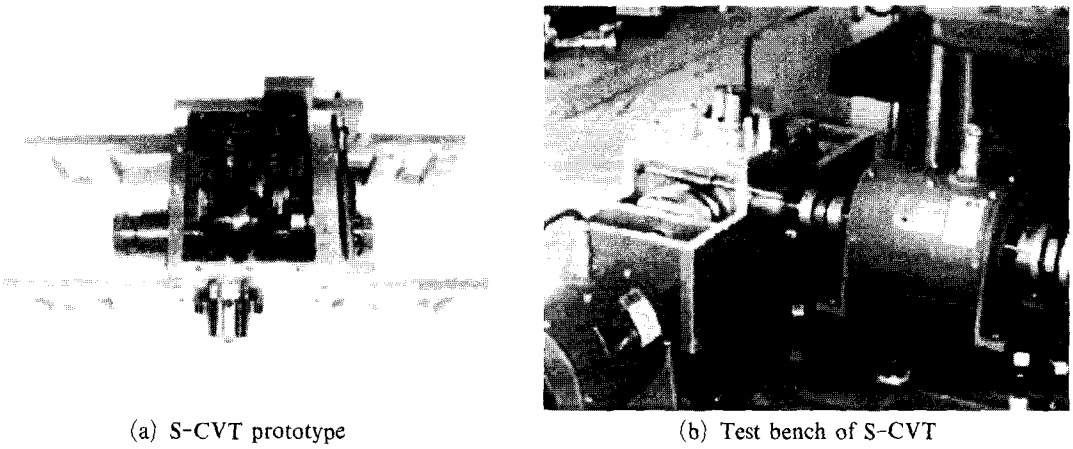

(a) S-CVT prototype (b) Test bench of S-CVT

Fig. 3 S-CVT and its test bench

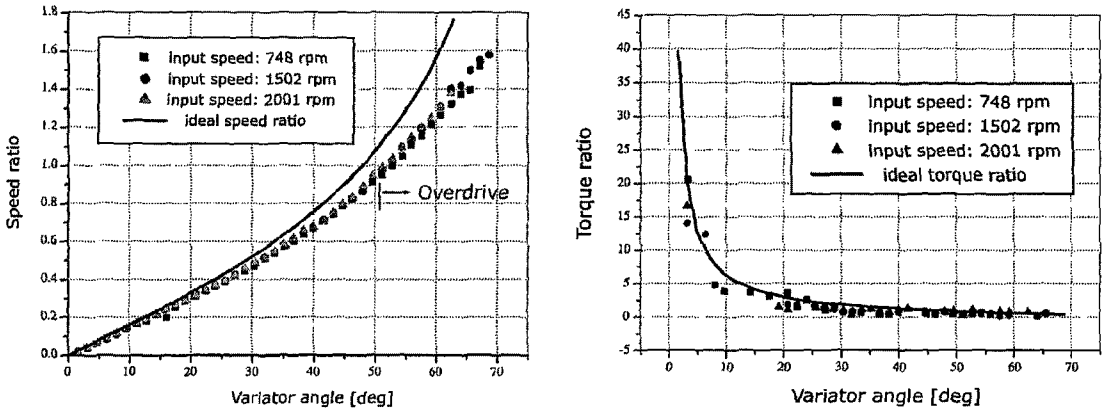

(a) Speed ratio of S-CVT (b) Torque ratio of S-CVT

Fig. 4 Experimental results

small-scale machine tools, and other applications with moderate power transmission requirements. Thus a DC motor was considered here as the power source.

DC motors are designed to be very efficient at their rated speeds, and it is now generally believed that there is very little room for improvement in terms of hardware performance. With recent advances in power electronics, the motor drivers that supply the input voltage or current are also now extremely efficient, compared to previously used analog drivers, enough to be used as variable speed drives (Werner, 1996; Kassankian et al., 1991). In addition, dc motor optimal control algorithms that take into account the load and other operating characteristics have been developed (Tadashi, 1990; Parviz and Wils, 1994), further reducing overall power consumption.

3.1 Equations of motion

We now consider a general armature-controlled dc motor as shown in Figure 5, in which the field current is held constant. We adopt the following nomenclature:

R_a=armature resistance [ohm]
L_a=armature inductance henry]
i_a=armature current [ampere]
i_f=field current {ampere]
e_a=applied armature voltage [volt]
e_b=back-emf (electromotive force) [volt]
ω_M=angular velocity of the motor [rad/sec]
ω_o=angular velocity of the CVT output shaft [rad/sec]
I_{eq}=equivalent moment of inertia of the motor and load referred to the motor shaft [kg·m^2]
T_M=motor torque [N·m]
T_{load}=load torque [N·m]

Then the circuit equation is

$$L_a\frac{di_a}{dt}+R_ai_a+e_b=e_a \tag{3}$$

The induced voltage e_b is directly proportional to the speed of the motor ω_M, or

$$e_b=k_e\omega_M \tag{4}$$

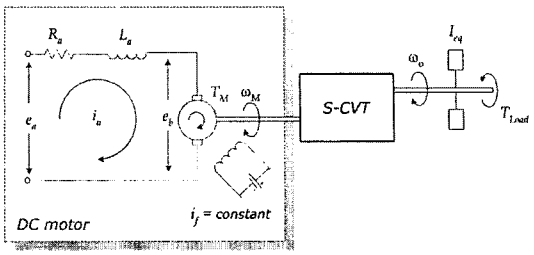

Fig. 5 Diagram of an armature-controlled dc motor

where k_e is a back emf constant. The motor torque T_M is directly proportional to the armature current:

$$T_M=ki_a \tag{5}$$

where k is a motor-torque constant.

Referring to Figure 5, we consider an S-CVT equipped power transmission. Using a gear train including CVTs at the motor shaft has the effect of reducing not only the load torque by the gear ratio, but also the equivalent inertia by a square of the gear ratio; the motor dynamic equation becomes

$$\frac{I_{eq}}{\alpha^2}\frac{d\omega_M}{dt}=T_M-\frac{T_{Load}}{\alpha},\ \omega_o=\omega_M\frac{1}{\alpha} \tag{6}$$

where α represents the reduction gear ratio. In the case of the S-CVT, however, α is replaced by the torque ratio of the S-CVT, i.e., $\alpha=\cot\theta$, so that the motor dynamic equation becomes

$$I_{eq}\tan^2\theta\frac{d\omega_M}{dt}=T_M-T_{Load}\tan\theta,\ \omega_o=\omega_M\tan\theta \tag{7}$$

Assuming that the armature inductance L_a in the circuit is small enough to neglect, we obtain the following equation from (3):

$$R_ai_a+e_b=e_a$$

thus the motor torque can be written as

$$T_M=\frac{k(e_a-k_e\omega_M)}{R_a} \tag{8}$$

Finally, the differential equation for the speed of the output shaft ω_o (7) becomes

$$I_{eq}\frac{d\omega_o}{dt}+\frac{kk_e}{R_a}\omega_o\cot^2\theta=\frac{ke_a}{R_a}\cot\theta-T_{Load} \tag{9}$$

3.2 Power efficiency of a DC motor

In this subsection, we consider the efficiency

characteristics of a general armature-controlled dc motor in Figure 5. The torque produced by a dc motor is directly proportional to the armature current (5); when the equivalent inertia and/or the load torque applied at the motor shaft is increased, the armature current must also be increased.

Rearranging the above equations and using the fact that the value of k_e is equal to k, the relationship between the mechanical power and the electric power is

$$T_M\omega_M = e_a i_a - i_a^2 R_a \tag{10}$$

In the above equation, the $i_a^2 R_a$ term represents the electric power-loss, called the armature-winding loss, generally dissipated through heat generation.

From Equation (3), at certain values of the armature voltage, decreasing the armature current will increase the value of the back-emf and the motor speed. Based on these observations, one can notice that motors have their highest efficiency in the low-torque, high-speed region. Figure 6 depicts the power efficiency of a general dc motor with respect to the motor speed and the load torque. As can be seen from the graph, motor efficiency is highest in the low-torque, high-speed region (indicated in dark blue), with the efficiency dropping off steeply in other regions. To enhance the power efficiency of a dc motor, it is clearly advantageous to operate it in this region of maximum efficiency.

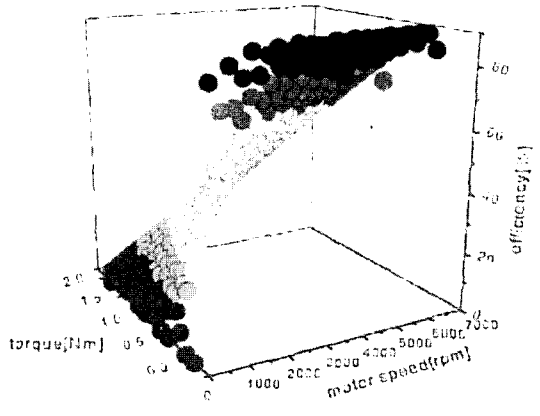

Fig. 6 Efficiency of an armature-controlled dc motor

4. Minimum Energy Control via a B-Spline Parameterization

In this section, we describe the minimum energy control design via a B-Spline parameterization. The minimum energy control problem of an S-CVT equipped power transmission is defined as follows:

Find the optimal control u that

$$\text{minimizes } J=\int_{t_0}^{t_f} i_a e_a dt \tag{11}$$

$$\text{subject to } I_{eq}\dot{\omega}_o = -\frac{kk_e}{R_a}\omega_o u^2 + \frac{ke}{R_a}u - T_{Load}$$

where u is the gear ratio, i.e., $\cot\theta$. The boundary conditions can be expressed in various forms according to the target performance. In this section, we consider the more complicated case of the S-CVT application for some position changers, e.g. a mobile robot, a vehicle, a positioning table, etc. For this case, the boundary conditions are given as follows:

$$\omega_o(t_0)=\omega_o(t_f)=0,\ s(t_0)=0,\ s(t_f)=d$$

where d is the desired displacement, $s(t)$ represents the displacement profile, and t_o, t_f represent the initial and final times respectively.

4.1 B-Spline parameterization

A solution to the above optimal control can be found by assuming that the displacement profile $s(t)$ is parameterized by a B-spline. The B-spline curve depends on the basis functions $B_i(t)$ and the control points $\mathbf{p}=[p_1, \cdots, p_n]$ with $p_i \in \mathrm{R}$. The displacement profile then has the form $\mathbf{s}=s(t, \mathbf{p})$ with

$$s(t, \mathbf{p}) = \sum_{i=1}^{n} B_i(t)\, p_i \tag{12}$$

Using this formulation (12), ω_o, $\dot{\omega}_o$ and u, which are functions of t and $\mathbf{p}$, can be written as

$$\omega_o(t, \mathbf{p}) = \frac{1}{r}\frac{\partial}{\partial t} s(t, \mathbf{p})$$

$$\dot{\omega}_o(t, \mathbf{p}) = \frac{1}{r}\frac{\partial^2}{\partial t^2} s(t, \mathbf{p})$$

and

$$u(t, \mathbf{p}) = \frac{ke_a + \sqrt{D(t, \mathbf{p})}}{2kk_e\omega_o} \tag{13}$$

where $D(t, \mathbf{p}) = k^2e_a^2 - 4R_akk_e\omega_o(T_{Load} - I_{eq}\omega_o)$, r is the conversion factor from a rotational speed into a linear speed (for the cases of mobile robots and vehicles this means the wheel radius). The control u is determined from Equation (13), but an additional inequality constraint $D(t, P) \geq 0$, $\forall t \in [t_0, t_f]$ must also be satisfied. In order to satisfy the boundary conditions, we set p_1, p_2 to zero and p_{n-1}, p_n to d.

Setting the input voltage e_a to a constant value, the armature current i_a can be calculated from Equations (7) and (8):

$$i_a(t, \mathbf{p}) = \frac{e_a - k_e\omega_o u}{R_a}$$

Hence the original optimal control problem is converted into a parameter optimization problem as follows:

$$\begin{aligned} &\textit{minimize } J(\mathbf{p}) = e_a \int_{t_0}^{t_f} i_a(t, \mathbf{p})\, dt \\ &\textit{subject to } D(t, \mathbf{p}) \geq 0,\ \forall t \in [t_0, t_f] \end{aligned} \tag{14}$$

4.2 Gradients of the objective function and constraint

To apply various parameter optimization algorithms (i.e., steepest descent, modified Newton method, quasi-Newton method, penalty method, etc.) to this problem (14), we must formulate the gradients of the objective function and constraint because almost all optimization algorithms require gradients of the objective function and constraint.

The gradient of the objective function is

$$\frac{\partial J}{\partial p_i} = \int_{t_0}^{t_f} \frac{\partial i_a}{\partial p_i} e_a dt$$

where the partial derivatives of i_a are as follows:

$$\frac{\partial i_a}{\partial p_i} = -\frac{k_e}{R_a}\left(\frac{\partial \omega_o}{\partial p_i} u + \omega_o \frac{\partial u}{\partial p_i}\right)$$

The derivatives of ω_o are obtained from the fact that

$$\frac{\partial \mathbf{s}}{\partial p_i} = B_i(t)$$

Since the constraint in Equation (14) is represented in the form of inequality, we can just know whether the constraint is effective or ineffective. In order to find the gradient of the constraint, we now propose the new constraint by defining a new function, $g(t, \mathbf{p})$, $\tilde{g}(\mathbf{p})$, as follows:

$$g(t, \mathbf{p}) = \begin{cases} -D(t, \mathbf{p}) & \text{if } D(t, \mathbf{p}) < 0 \\ 0 & \text{if } D(t, \mathbf{p}) \geq 0 \end{cases}$$

$$\tilde{g}(\mathbf{p}) = \int_{t_0}^{t_f} g(t, \mathbf{p})\, dt$$

Figure 7 illustrates the interpretation of $\tilde{g}(\mathbf{p})$. With these definitions, it is apparent that the constraint in Equation (14) is equivalent to the following constraint:

$$\tilde{g}(\mathbf{p}) = 0$$

It is difficult to solve this constraint analytically; however the gradient is well defined. $\tilde{g}(\mathbf{p})$ can be redefined as

$$\tilde{g}(\mathbf{p}) = \sum_j \int_{\alpha_j}^{\beta_j} -D(t, \mathbf{p})\, dt$$

where $D(t, \mathbf{p}) < 0$ for $\forall t \in [\alpha_j, \beta_i]$ and $D(\alpha_j, \mathbf{p}) = D(\beta_j, \mathbf{p}) = 0$. The gradient of $\tilde{g}(\mathbf{p})$ can be defined as follows:

$$\begin{aligned} \frac{\partial \tilde{g}}{\partial p_i} &= \sum_j \frac{\partial}{\partial p_i} \int_{\alpha_j}^{\beta_j} -D(t, \mathbf{p})\, dt \\ &= \sum_j \left(\int_{\alpha_j}^{\beta_j} -\frac{\partial D(t, \mathbf{p})}{\partial p_i} dt - D(\beta_j, \mathbf{p}) \frac{\partial \beta_j}{\partial p_i} + D(\alpha_j, \mathbf{p}) \frac{\partial \alpha_j}{\partial p_i} \right) \\ &= \sum_j \int_{\alpha_j}^{\beta_j} -\frac{\partial D(t, \mathbf{p})}{\partial p_i} dt \end{aligned}$$

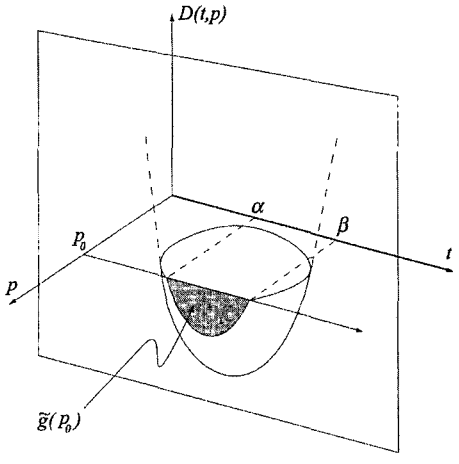

Fig. 7 Interpertation of $\tilde{g}(\mathbf{p})$

The gradient is now rewritten as follows:

$$\frac{\partial g}{\partial p_i}=\begin{cases}-\dfrac{\partial D(t,\mathbf{p})}{\partial p_i} & \text{if } D(t,\mathbf{p})<0\\ 0 & \text{if } D(t,\mathbf{p})\geq 0\end{cases} \tag{15}$$

$$\frac{\partial \tilde{g}(\mathbf{p})}{\partial p_i}=\int_{t_0}^{t_f}\frac{\partial g(t,\mathbf{p})}{\partial p_i} \tag{16}$$

Because it is difficult to find α_j, β_j for a given $\mathbf{p}$, we can alternatively use Equation (16) to numerically calculate the gradient of the constraint.

5. Energy Savings Using Optimal Control

We determine by simulation the power consumption for a minimum energy control and a comparative control. To benchmark the optimal control, we first design a control based on *the computed torque control method* which is used widely in robotics and other engineering fields. The computed torque control compensates for tracking errors by using feedback information about the differences between the predefined objective trajectories of position, speed, acceleration and the estimated actual trajectories.

From the given output speed profile $\omega_o(t)$, the computed motor torque T_M is calculated using Equation (8) and the relation of ω_o between ω_M:

$$T_M=\frac{k}{R_a}(e_a-k_e\omega_o\cot\theta)$$

This motor torque must be balanced by the torque due to the equivalent inertia and the load (7), i.e.,

$$\frac{k}{R_a}(e_a-k_e\omega_o\cot\theta)=\left(I_{eq}\frac{d\omega_o}{dt}+T_{Load}\right)\tan\theta$$

Rearranging the above equation yields

$$\frac{kk_e}{R_a}\omega_o\cot^2\theta-\frac{ke_a}{R_a}\cot\theta+I_{eq}\frac{d\omega_o}{dt}+T_{Load}=0 \tag{17}$$

Hence the variator angle profile can be obtained by solving the second-order polynomial Equation (17). The comparative control is designed to manipulate the output speed in a sinusoidal fashion, satisfying the boundary conditions. To satisfy the boundary conditions the displacement profile is described as follows:

$$s(t)=\frac{d}{2}\left(1-\cos\frac{\pi t}{t_f}\right)$$

From this relation, ω_o, $\dot{\omega}_o$ are derived by differentiation, and the control u is obtained from Equation (17). We assign the final time t_f to be 5 *seconds*, and the desired displacement d to be 8 *meters*. For the numerical investigation, we assign a load torque T_{Load} of 0.07 Nm, and an equivalent inertia with respect to the input shaft I_{eq} of 0.01 kgm^2; for these values, the stall torque is calculated to be 1.6 Nm. We therefore choose a dc motor with a power rating of 60 Watts (see Table 1 for the detailed specifications of the dc motor).

Based on the mathematical models, we have developed a simulation program with MATLAB. This program uses Simpson's rule for integration and the BFGS quasi-Newton method for optimization. Figure 8 depicts the corresponding variator angle time trajectories which are directly related with the controls for each case. In this figure, the optimized variator angle is much flatter than in the case of the computed torque control. The resulting motor speed and torque are calculated in Figure 9 As can be seen in Figure 9, in the minimum energy control case the variation of the motor speed is smaller and the motor torque

Table 2 Characteristic coefficients of dc motor

Rated voltage	12 Volts
Motor-torque constant	0.0272 N·m/A
Back emf constant	0.0272 volt·sec/rad
Rotor winding resistance	0.48 Ohm

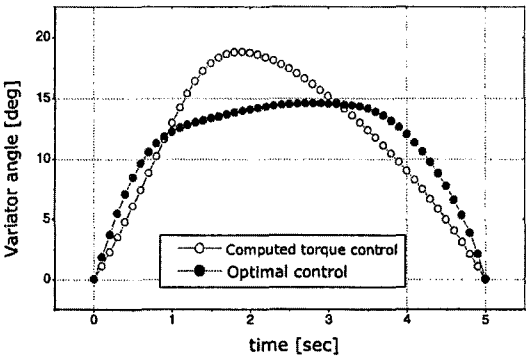

Fig. 8 Optimal variator angle time profile

is closer to zero compared to the other controller.

Figure 10 shows the output behavior of the S-CVT equipped power transmission. From this figure, one can see that the minimum energy controller accelerates the output faster than the computed torque control.

The consumed energy for each case is calculated using the above results and the relation

$$Energy = \int | e_a(t) \times i_a(t) | \, dt$$

We regard negative values of current and voltage as part of the overall consumed energy. Consequently, we have calculated the energy consumption in Table 2. The optimized energy consumption is less than that of the other case by almost 24.1%.

Table 2 Energy consumption with the minimum energy control

Minimum energy control	Computed torque contro
43.37 Joules	57.16 Joules

6. Conclusion

In this paper, we have presented the minimum energy control law of S-CVT connected to a dc motor. The S-CVT can realize the infinitely variable transmission characteristics. And its compact and simple design and its relatively simple control make it particularly effective for mechanical systems in which excessively large torques are not required. Such S-CVT equipped power transmission has the advantage of being able to operate the motors in their regions of maximum efficiency, thereby improving the energy efficiency of the transmission system.

We first review the structure and operating principles of the S-CVT, including experimental

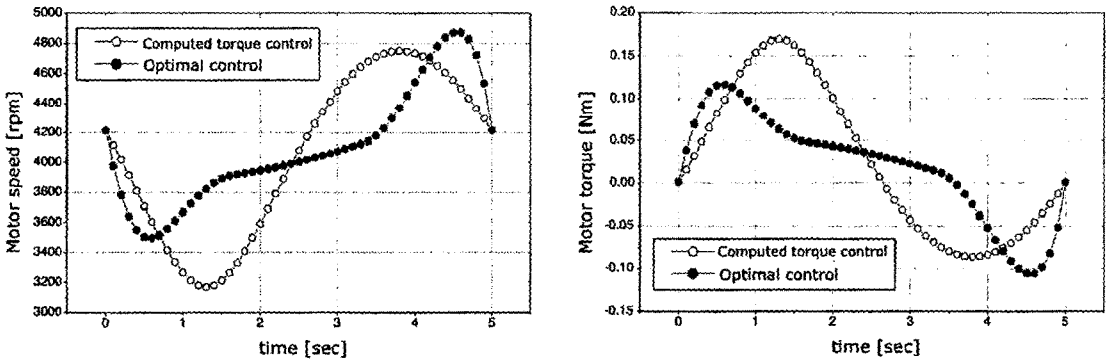

(a) Motor speed (b) Motor torque

Fig. 9 Motor behaviors with the minimum energy control

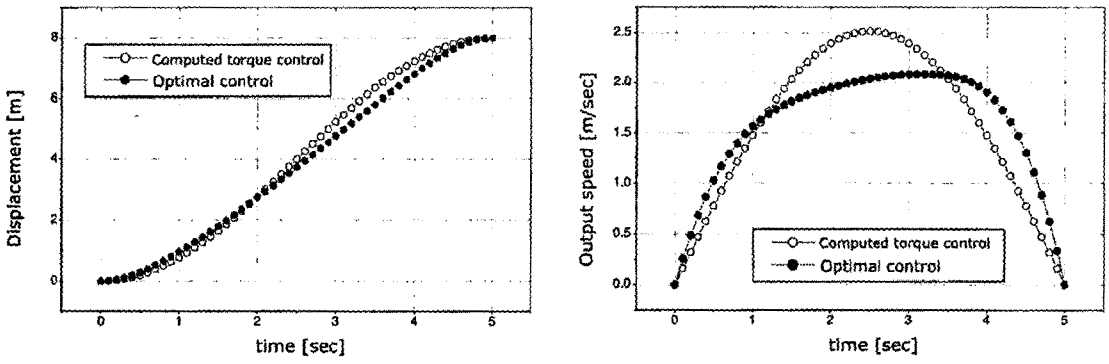

(a) Displacement (b) Output speed

Fig. 10 Output behaviors with the minimum energy control

results of its performance. And then using an ideal motor model, we carried out a dynamic analysis of an S-CVT equipped power transmission system, and described the power efficiency characteristics of a DC motor. And we describe a minimum energy control law of S-CVT connected to a dc motor. The minimum energy control design is carried out via B-spline parameterization. By parameterizing the displacement profile in terms of a B-spline, the optimal control problem is converted into a parameter optimization problem involving the B-spline control points. Finally, we present computer simulation results using an optimal control law benchmarked with a computed torque control algorithm for S-CVT to show the effectiveness of the developed minimum energy control law.

Acknowledgment

This research was supported in part by the Korea Research Foundation made in the program year 2003.

References

Proc. of Inter. Conf. on Continuously Variable Power Transmissions CVT '96, Society of Automotive Engineers of Japan, Yokohama, Sept. 11-12, 1996.

Proc. of Inter. Congress on Continuously Variable Power Transmissions CVT '99, Sponsored by I Mech E, JSAE, KIVI, SAE, VDI-EKV, Eindhoven, Sept. 16-17, 1999.

Proc. of the 7th Inter. Power Transmission and Gearing Conference, Design Engineering Division, ASME, San Diego, California, Oct. 6-9, 1996.

Heera Lee and Hyunsoo Kim, 2002, "Optimal Engine Operation by Shift Speed Control of a CVT," in *KSME International Journal*, pp. 882~888, Vol. 16, Issue 7, KSME.

Jungyun Kim, Hanjun Yeom, Park, F. C., Park, Y. I. and Munsang Kim, 2000, "On the Energy Efficiency of CVT-Based Mobile Robots," in *Proceedings of IEEE International Conference on Robotics and Automation*, pp. 1539~1544, Vol. 1, April 24-28, San Francisco, CA, U.S.A.

Jungyun Kim, Park, F. C., Yeongil Park, and Shizou, M., 2002, "Analysis and Control of a Spherical Continuously Variable Transmission," in *Journal of Mechanical Design*, pp. 21~29, Vol. 124, Issue 1, ASME.

Kassankian, J. G., Schlecht, M. F. and Verghese, G. C., 1991, *Principles of Power Electronics*, Cambridge, MA, Addison-Wesley, Chapter 1-8.

Parviz Famouri and Wils L. Cooley, 1994, "Design of DC Traction Motor Drives for High Efficiency Under Accelerating Conditions," *IEEE Transactions on Industry Applications*, Vol. 30, No. 4, July/August.

Tadashi Egami, Hideaki Morita and Takeshi Tsuchiya, 1990, "Efficiency optimized Model Reference Adaptive Control System for a dc Motor," in *IEEE Transactions on Industrial Electronics*, Vol. 37, No. 1, February.

Takahashi, S., 1998, "Fundamental Study of Low Fuel Consumption Control Scheme Based on Combination of Direct Fuel Injection Engine and Continuously Variable Transmission," in *Proc. of the 37th IEEE Conf. on Decision and Control*, pp. 1522~1529, Tampa, Florida.

Werner Leonhard, 1996, *Control of Electrical Drives*, 2nd Ed., Springer.